SUPPORTING INFORMATION

The quantum dot *vs.* organic dye conundrum for ratiometric FRET-based biosensors: which one would you chose?

Chloé Grazon[a, b, c,] * , Margaret Chern[d] , Pat Lally[f] , R C. Baer[e, g] , Andy Fan[f] , Sébastien Lecommandoux[b] , Catherine Klapperich[f] , Allison M. Dennis[d, f] *, James E. Galagan[e, f, g] * , Mark W. Grinstaff [a, d, f] *

[a] Department of Chemistry, Boston University, Boston, MA 02215, USA

[b] Univ. Bordeaux, CNRS, Bordeaux INP, LCPO, UMR 5629, F-33600, Pessac, France

[c] Univ. Bordeaux, CNRS, Bordeaux INP, ISM, UMR 5255, F-33400 Talence, France

[d] Division of Materials Science and Engineering, Boston University, Boston, MA 02215, USA

[e] Department of Microbiology, Boston University, Boston, MA 02118, USA

[f] Department of Biomedical Engineering, Boston University, Boston, MA 02215, USA

[g] National Emerging Infectious Diseases Laboratories, Boston University, Boston, MA 02118, USA

Emails: chloe.grazon@u-bordeaux.fr / aldennis@bu.edu / jgalag@bu.edu / mgrin@bu.edu

Oligonucleotides

Table S1 DNA sequences used in this study

DNA	Abbreviation	Sequence 5'→3'
DNA1 Texas Red	DNA1-TR	TR-GCCTAACTAGCCGTTCGGCTAGTTATTC
DNA2 Texas Red	DNA2-TR	TR-GCCTAACTAGCCGTTCGGCAAGTAATTC
DNA1 Cyanine5	DNA1-Cy5	Cy5-GCCTAACTAGCCGTTCGGCTAGTTATTC-Cy5
DNA2 Cyanine5	DNA2-Cy5	Cy5-GCCTAACTAGCCGTTCGGCAAGTAATTC-Cy5
Comp. of DNA1	CsDNA1-TR	GAATAACTAGCCGAACGGCTAGTTAGGC
	CsDNA1-Cy5	
Comp. of DNA2	CsDNA2-TR	GAATTACTTGCCGAACGGCTAGTTAGGC
	CsDNA2-Cy5	
Scrambled DNA Texas Red	DNAsbd-TR	TR-TGTGCGTGTCCCTCGCTCGGTTTCACGA
Scrambled DNA Cyanine5	DNAsbd-Cy5	Cy5-TGTGCGTGTCCCTCGCTCGGTTTCACGA-Cy5
Comp. of scrambled DNA	CsSbd-TR	TCGTGAAACCGAGCGAGGGACACGCACA
	Cs Sbd-Cy5	
DNA1-azide	DNA1-N$_3$	N$_3$-TTTTAACTAGCCGTTCGGCTAGTT
Comp. of DNA1-N3	CsDNA1-N$_3$	AACTAGCCGAACGGCTAGTT
DNA2-azide	DNA2-N$_3$	N$_3$-TTTT AAC TAG CCG TTC GGC AAG TA
Comp. of DNA2-N3	CsDNA2-N$_3$	TA CTT GCC GAA CGG CTA GTT
Scrambled DNA-azide	Sbd-N$_3$	N$_3$-TTTTCGTGTCCCTCGCTCGGTTTC
Comp. of Scrambled DNA-azide	CsSbd-N$_3$	GAAACCGAGCGAGGGACACG

Table S2. Affinity and kinetic measurements associated with aTF binding to DNA in the absence of sterols, measured by BLI.

Protein	DNA	K_D (M)	K_D Error (M)	k_{on} ($M^{-1}s^{-1}$)	k_{on} Error ($M^{-1}s^{-1}$)	k_{off} (s^{-1})	k_{off} Error (s^{-1})
SRTF1	DNA1	4.47E-09	3.43E-10	1.70E+05	9.45E+03	7.59E-04	3.99E-05
	DNA2	7.11E-09	5.18E-10	1.94E+05	1.15E+04	1.38E-03	5.92E-05

Data analysis

Dose-response curve fits
Raw dose-response curves were obtained by plotting F_A/F_D as a function of the progesterone concentration and fitted with the non-linear Hill equation:

$$y = A_2 + \frac{A_1 - A_2}{1 + (\frac{x}{IC50})^p}$$

Eq. S1

where IC50 is the half maximal inhibitory concentration.

Sensor output is the normalization of the fluorescent spectra of the donor and acceptor according to the following equation:

$$\text{Sensor output} = \frac{F_i - F_{max}}{(F_{min} - F_{max})}$$

Eq. S2

Were $F = F_A/F_D$, F_i is for [PRG] = i, F_{min} stands for the average on 3 experiments of F for [PRG] = 0 nM and Fmax stands for the average on 3 experiments of F for [PRG] = 10 μM.

Limit of detection calculation
The detection limit is the smallest concentration or absolute amount of analyte that has a signal significantly larger than the signal arising from a reagent blank. Mathematically, the limit of detection in the signal domain (L_D) is given by:

$$L_D = mean_{blank} - 3.3 \times \sigma_{test}$$

Eq. S3

where $mean_{blank}$ is the mean signal for a reagent blank and σ_{test} is the pool standard deviation for all test samples in the dilution series, calculated as [1]:

$$\sigma_{test} = \sqrt{\frac{\sum_{i=1}^{m} \sigma_i^2}{m}}$$

Eq. S4

where σ_i is the standard deviation in signal intensities for n replicates of the ith test concentration, with a total of m different test concentrations.

The limit of detection (LOD) was calculated using the parameters of the fit with the non-linear equation for $y = L_D$:

$$LOD = IC_{50} \times \sqrt[p]{\frac{A_1 - A_2}{L_D - A_2} - 1}$$

Eq. S5

The 95% Confidence Interval was calculated using Origin Pro Software.

Fluorescent protein characterization
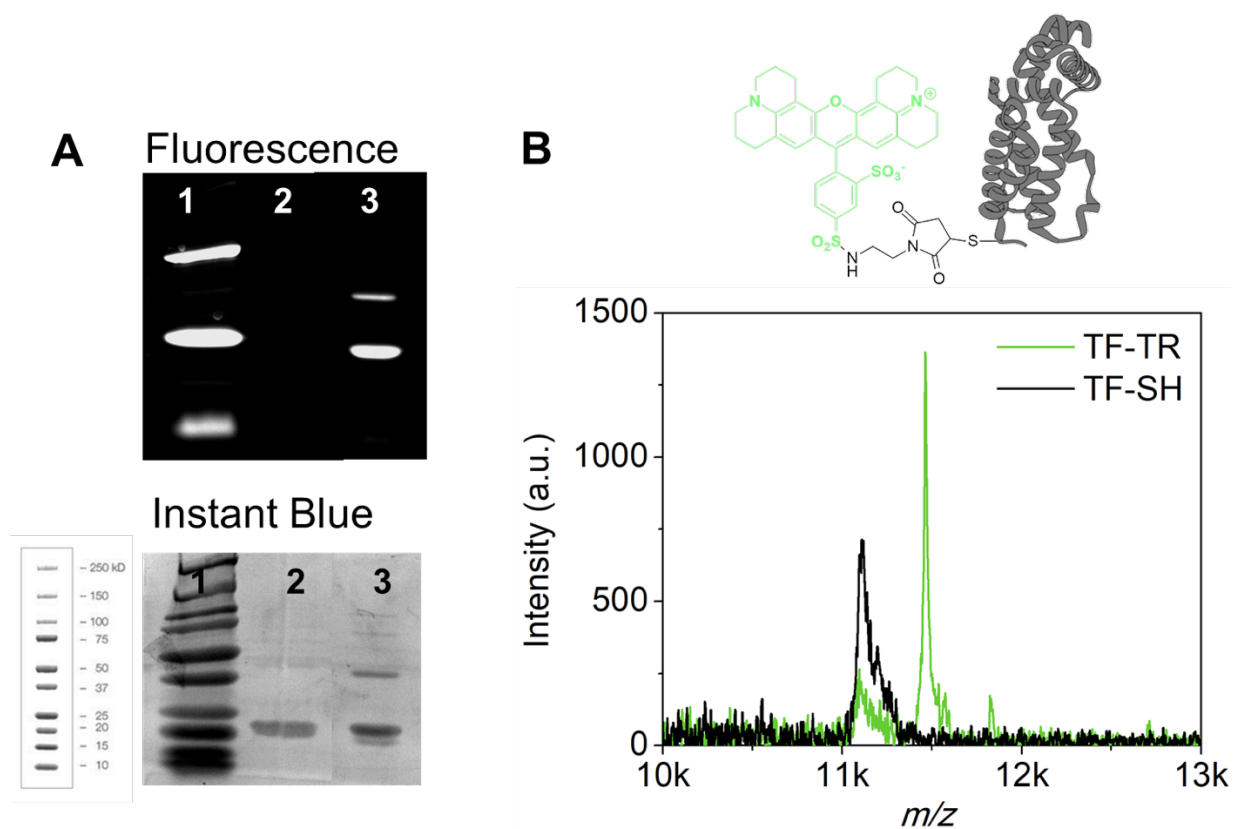
Figure S1. SRTF1-Texas Red Characterization. A. 12% SDS-PAGE gels revealed by fluorescence (top) and stained with instant blue (below). Line 1: protein ladder, 2: SRTF1-SH, 3: SRTF1-TR after purification. The upper band on line 3 correspond to the protein dimer (MW = 2×22.3 kD). B. MALDI-TOF spectra of SRTF1-SH (for z = 2, m/z = 11107) and SRTF1-TR (for z = 2, m/z = 11463).

Efficiency of TF-TR grafting was confirmed by absorption measurements:

- Absorption of TF-TR at 595 nm indicates a concentration after purification of 33 μMTexas Red (using εTexas Red = 85,000M^{-1}cm^{-1} at 595nm).

- The same sample was analyzed using a Bradford assay yielding a [protein] = 37μM.

We thus estimated that around 90% of the protein was conjugated with Texas Red.
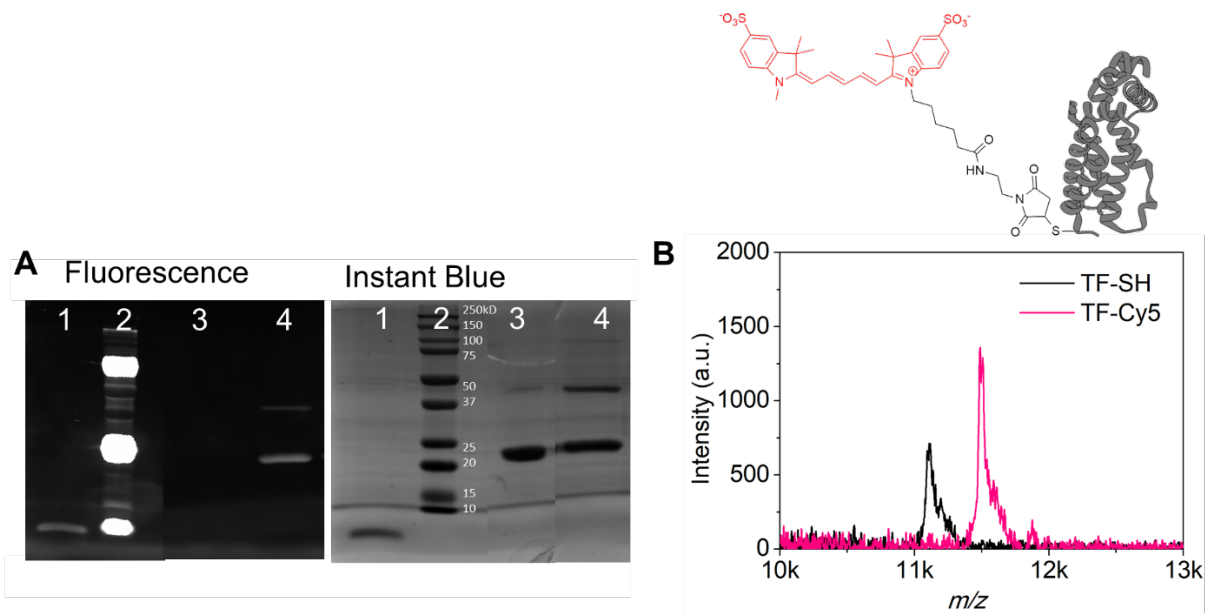
Figure S2. SRTF1-Cy5 Characterization. A. 12% SDS-PAGE gels revealed by fluorescence (left) and stained with instant blue (right). Line 1: Cy5 dye, 2: protein ladder, 3: SRTF1-SH, 4: SRTF1-Cy5 after purification. The upper band on line 4 correspond to the protein dimer (MW = 2×22.3 kD). B. MALDI-TOF spectra of SRTF1-SH (for z = 2, m/z = 11107) and SRTF1-Cy5 (for z = 2, m/z = 11494).

Quantum Dots
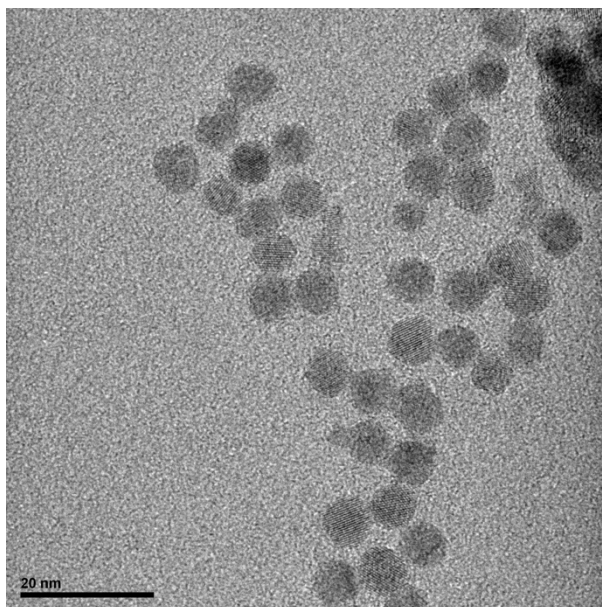
Figure S3. TEM images of the QD in chloroform. Scale bar: 20 nm.
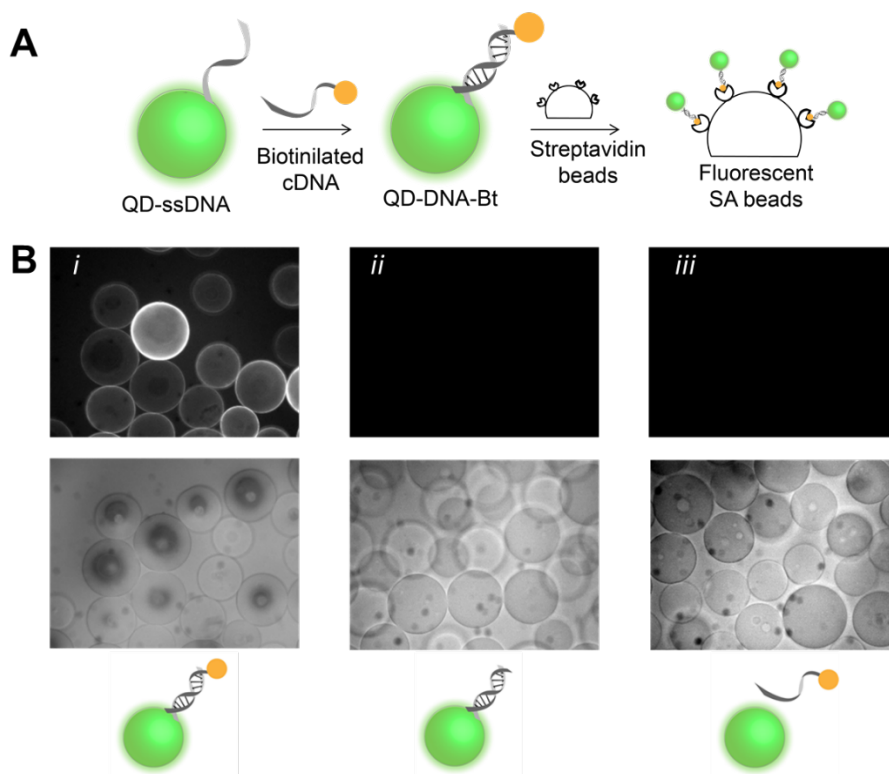
Figure S4. Grafting DNA-N_3 on QD-DBCO based on our previous work (C. Grazon, M. Chern *et al.,* Chem Commun. 2019)[2]. A. Scheme of the copper-free click reaction between QD@P-DBCO + DNA-N_3 and hybridization of the QD-ssDNA with its biotinylated complement. The QD-dsDNA-bt can be pulled down on streptavidin (SA) beads to verify hybridization. B. Fluorescence images of agarose SA-beads incubated with i) QD decorated with DNA-N_3 hybridized with the biotinylated complement, ii) QD decorated with DNA-N_3 hybridized with a non-biotinylated complement, iii) QD-DBCO mixed with the biotinylated DNA complement.

Absorption and emisison spectra of the donors and acceptors
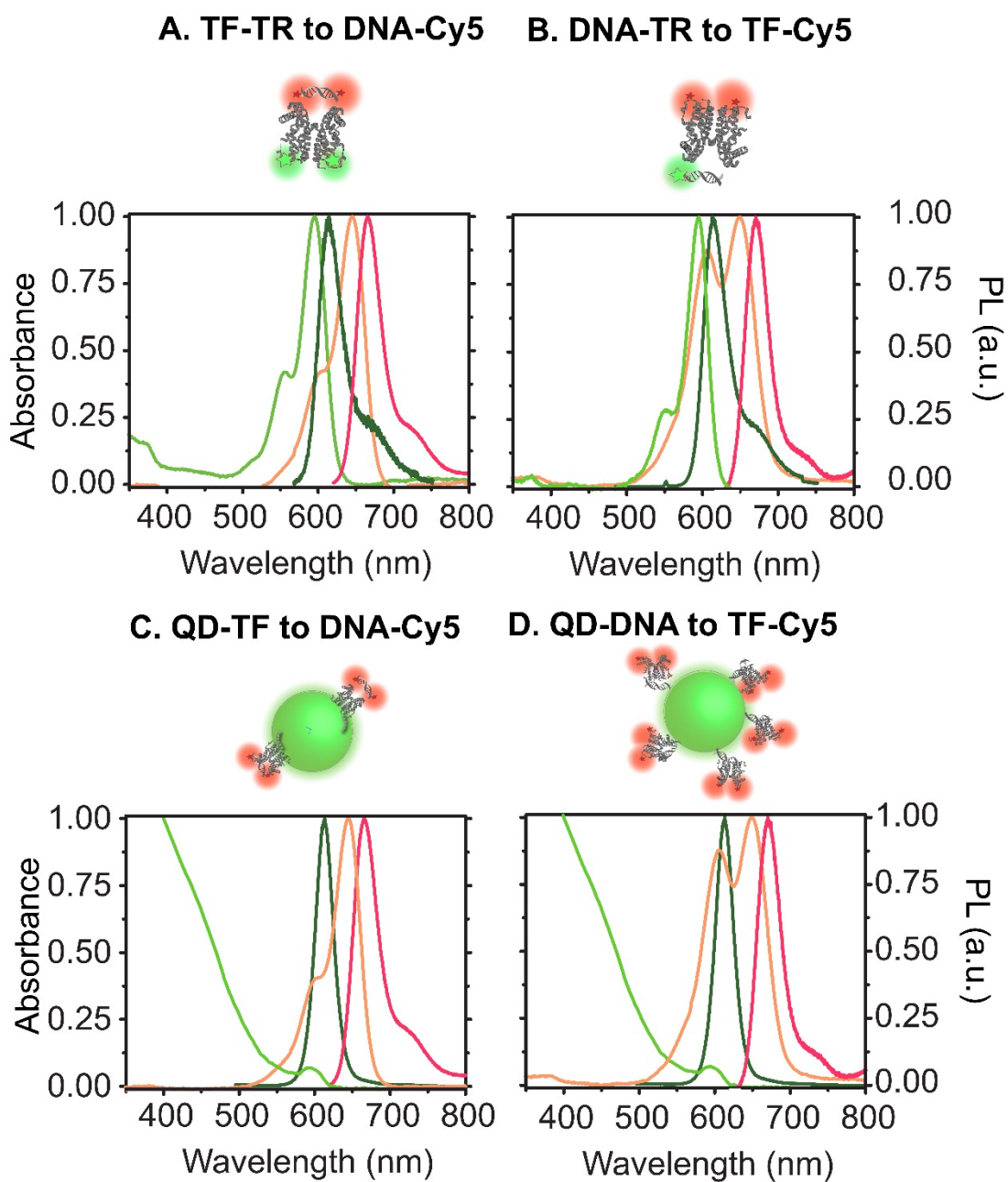
Figure S5. Normalized absorption and emission spectra of the different FRET pairs in 1x HEPES buffer. The donor spectra are represented in green and the acceptor spectra in pink. Absorbance spectra are lighter, while fluorescence spectra are darker in color.
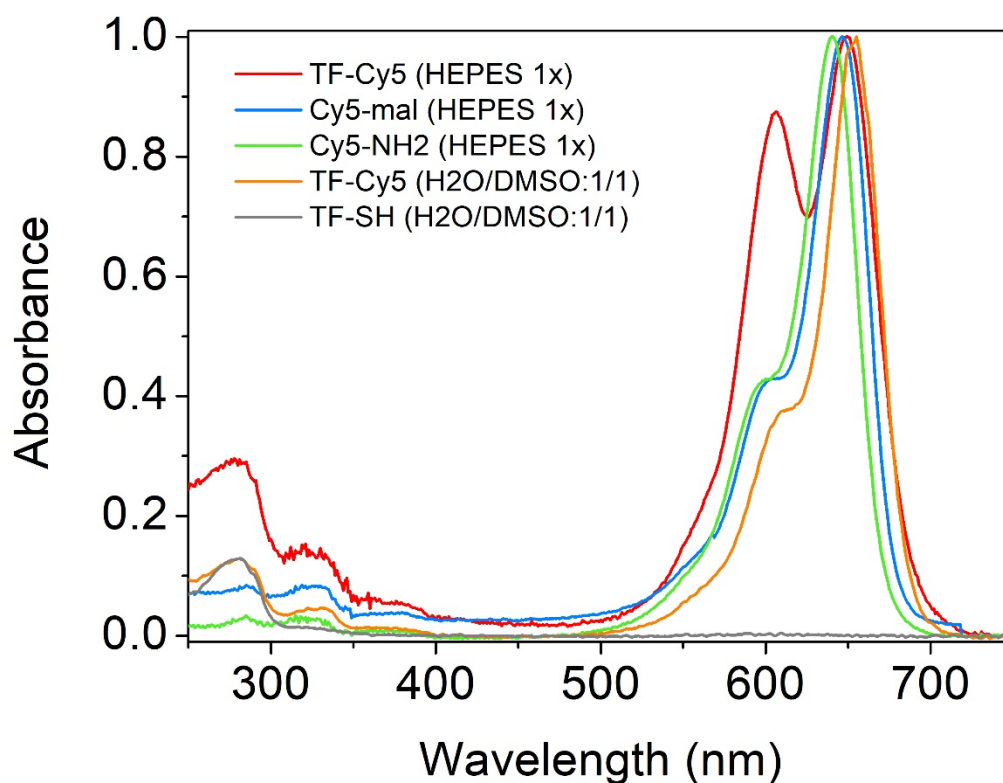
Figure S6. Normalized absorption spectra of different Cy5-labelled fluorophores. TF-Cy5 (red) in HEPES 1x shows a stronger vibrational shoulder in the $S_0 \rightarrow S_1$ absorption band than the reference dyes Cy5-maleimide (blue) or Cy5-amine (green) in the same conditions. When TF-Cy5 is diluted in a mixture of 1:1 DMSO:H_2O the vibrational shoulder decreases to recover the regular absorption spectra of a Cy5 dye.

Lifetime measurements
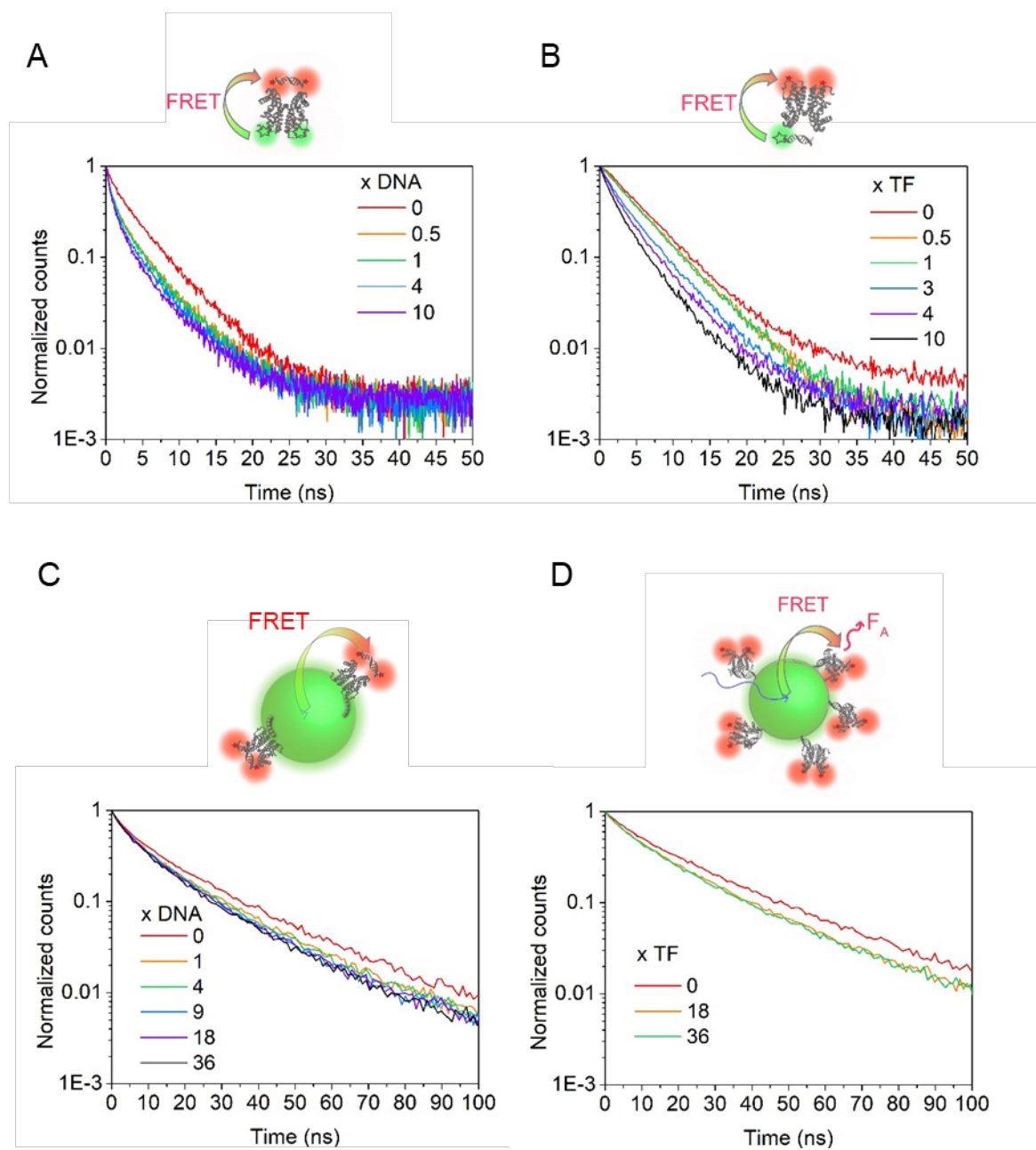
Figure S7. Lifetime measurements plotted on a semi-log scale, of the different FRET pairs with titration of the acceptor to the donor. For all the experiments, λ_{exc} = 405 nm and data are shown for DNA1. For system A: TF-TR to DNA-Cy5 λ_F = 615 nm; B: DNA-TR to TF-Cy5 λ_F = 615 nm; C: TF-QD to DNA-Cy5 λ_F = 613 nm; D: DNA-QD to TF-Cy5 λ_F = 613 nm.

Table S3: FRET assay lifetime fits. Fluorescence lifetime parameters from Eq. 1 and FRET efficiency (E) calculated according to Eq. 5.

Dye-dye biosensors

Donor	Acceptor	DNA	A/D[a]	τ_1 (ns)	A_1 (%)	τ_2 (ns)	A_2 (%)	τ_3 (ns)	A_3 (%)	τ (ns)	τ stdev	χ^2	E
TF-TR	DNA-Cy5	-	0	0.93	33	4.30	65	12.2	2	3.29	0.04	1.17	0
		DNA1	0.1	0.92	41	4.05	57	10.2	3	2.95	0.04	1.15	11
		DNA1	0.5	0.60	53	2.85	34	6.15	12	2.06	0.05	1.15	38
		DNA1	1	0.03	51	0.16	33	0.18	16	1.91	0.03	1.07	42
		DNA1	4	0.59	60	2.73	32	6.74	8	1.76	0.03	1.14	46
		DNA1	10	0.52	53	1.92	35	5.53	12	1.61	0.03	1.12	51
		DNA2	0.1	0.82	38	3.90	55	7.54	7	2.99	0.07	1.11	9.1
		DNA2	0.5	0.55	41	2.38	38	5.48	21	2.28	0.04	1.16	31
		DNA2	1	0.80	57	3.67	38	7.71	5	2.23	0.06	1.01	32
		DNA2	4	0.68	56	3.20	39	8.17	5	2.04	0.04	1.04	38
		DNA2	10	0.60	53	2.23	34	5.78	12	1.80	0.04	1.10	45
		sbd	1	0.56	22	2.50	40	5.29	38	3.14	0.05	1.17	4.6
		sbd	4	0.60	34	3.41	52	6.55	14	2.90	0.07	1.12	12
		sbd	10	0.84	42	3.54	46	6.46	13	2.79	0.09	1.14	15
DNA-TR	TF-Cy5	DNA1	0	5.07	100	34.4	0	0	0	5.12	0.01	1.067	0
		DNA1	0.5	4.93	99	14.9	1	0	0	4.99	0.02	1.052	2.4
		DNA1	1	4.61	97	10.6	3	0	0	4.78	0.04	1.064	6.5
		DNA1	3	2.21	48	5.25	52	0	0	3.79	0.04	1.148	26
		DNA1	4	1.88	56	4.93	44	0	0	3.22	0.03	1.13	37
		DNA1	10	1.79	65	4.76	35	0	0	2.82	0.03	1.156	45
		DNA2	0	0.68	-5	5.11	105	0	0	5.34	0.02	1.09	0.0
		DNA2	0.5	0.43	-6	5.01	105	29.8	0	5.33	0.05	0.92	0.3
		DNA2	3	2.06	33	5.10	67	0	0	4.09	0.04	1.108	23
		DNA2	4	1.29	20	3.67	54	6.03	26	3.80	0.29	1.12	29
		DNA2	10	1.02	30	3.19	58	6.49	12	2.93	0.08	1.141	45
		sbd	0	5.12	100	10.0	0	0	0	5.14	0.04	1.237	0.0
		sbd	1	5.08	100	32.8	0	0	0	5.12	0.02	1.065	0.4
		sbd	4	5.09	100	27.7	0	0	0	5.13	0.02	1.092	0.2
		sbd	10	5.11	100	57.0	0	0	0	5.16	0.06	1.149	-0.4

a: molar ratio of acceptor dye per donor dye

QD-dye biosensors

Donor	Acceptor	DNA	A/D[a]	DNA/TF	τ_1 (ns)	A_1 (%)	τ_2 (ns)	A_2 (%)	τ_3 (ns)	A_3 (%)	τ (ns)	τ stdev	χ^2	E
TF-QD*	DNA-Cy5	DNA1	0	0	7.00	51	22.9	48	92.1	1.0	15.4	0.4	1.30	0
		DNA1	1	0.25	6.32	54	20.8	46	124.6	0.5	13.5	0.3	1.30	12
		DNA1	4	1	5.74	50	18.6	48	65.5	1.4	12.8	0.4	1.25	17
		DNA1	9	2.25	6.31	57	19.6	42	97.2	0.6	12.5	0.3	1.27	19
		DNA1	18	4.5	5.98	54	18.5	45	79.5	0.9	12.3	0.4	1.20	20
		DNA1	36	9	4.89	49	16.5	49	57.0	1.9	11.6	0.4	1.15	24
		DNA2	1	0.25	5.49	47	19.0	51	67.4	1.6	13.4	0.4	1.19	13
		DNA2	4	1	5.30	49	18.6	50	76.2	1.1	12.7	0.3	1.26	18
		DNA2	9	2.25	5.61	53	18.6	46	84.2	0.8	12.2	0.3	1.22	21
		DNA2	18	4.5	5.87	55	18.6	44	74.9	1.0	12.2	0.3	1.21	21
		DNA2	36	9	5.99	58	19.2	41	91.4	0.7	12.0	0.3	1.29	22
		sbd	9	2.25	6.09	48	22.0	51	97.0	0.9	15.0	0.3	1.30	2.8
		sbd	18	4.5	5.85	49	21.9	50	93.8	0.9	14.7	0.3	1.34	4.7
		sbd	36	9	5.74	50	21.7	49	81.2	1.1	14.4	0.3	1.37	6.3
DNA-QDɫ	TF-Cy5	DNA1	0	-	8.87	41	26.8	57	92.7	1.3	20.2	0.5	1.07	0
		DNA1	18	1.1	6.85	39	21.6	58	65.1	2.8	17.0	0.6	1.20	16
		DNA1	36	0.6	7.19	44	21.8	54	69.0	2.2	16.4	0.5	1.27	19
		sbd	0	-	9.15	43	26.3	55	85.1	1.6	19.8	0.6	1.19	0
		sbd	36	0.6	9.21	49	26.2	50	98.1	1.1	18.7	0.6	1.26	6

a: molar ratio of acceptor dye per donor dye

* 4 TF per QD

ɫ 18 DNA per QD

Sensor response

TF-TR to DNA-Cy5
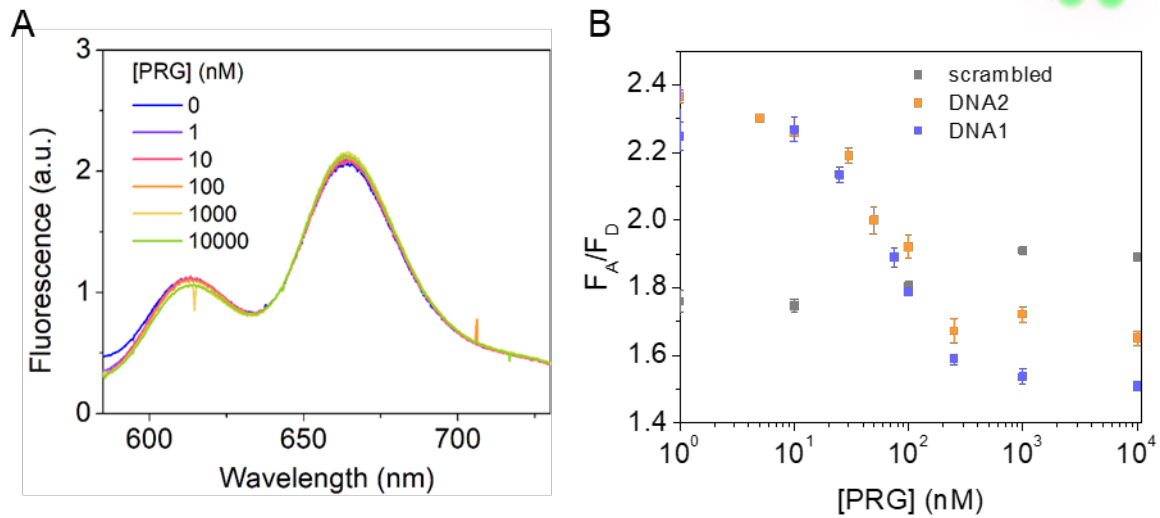
Figure S8. TF-TR to DNAsbd-Cy5 FRET sensor response using a scrambled DNA and a ratio TF-TR:DNA-Cy5=1:1. Left: fluorescence emission spectra (λ_{exc} = 550 nm) and right: dose-response curve upon PRG addition overlapped with the response of sensor A using DNA 1 and 2 in the same conditions. Data are mean ± standard deviation of n = 3.
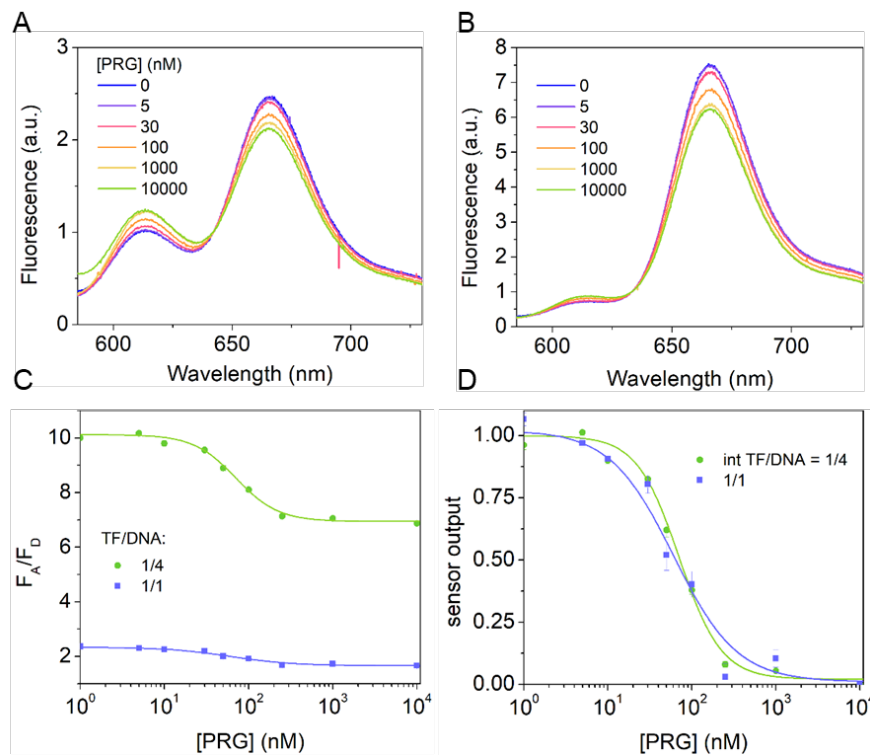
Figure S9. TF-TR to DNA2-Cy5 FRET sensor. A and B, fluorescence emission spectra (λ_{exc} = 550 nm) upon PRG addition with a ratio of TF-TR:DNA2-Cy5 =1:1 (A) and = 1:4 (B). C and D are the raw and normalized dose-response curve upon PRG addition. Data are mean ± standard deviation of n = 3.

13
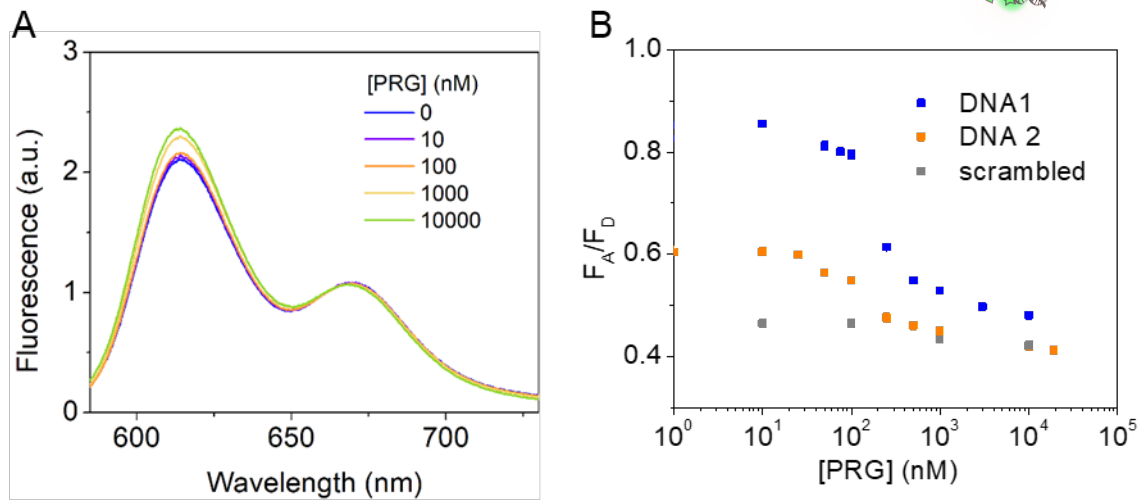
FRET

Figure S10. DNAsbd-TR to TF-Cy5 FRET sensor response using a scrambled DNA and a ratio DNAsbd-TR:TF-Cy5=1:4. Left: fluorescence emission spectra (λ_{exc} = 550 nm) and right: dose-response curve upon PRG addition overlapped with the response of sensor A using DNA 1 and 2 in the same conditions. Data are mean ± standard deviation of n = 3.
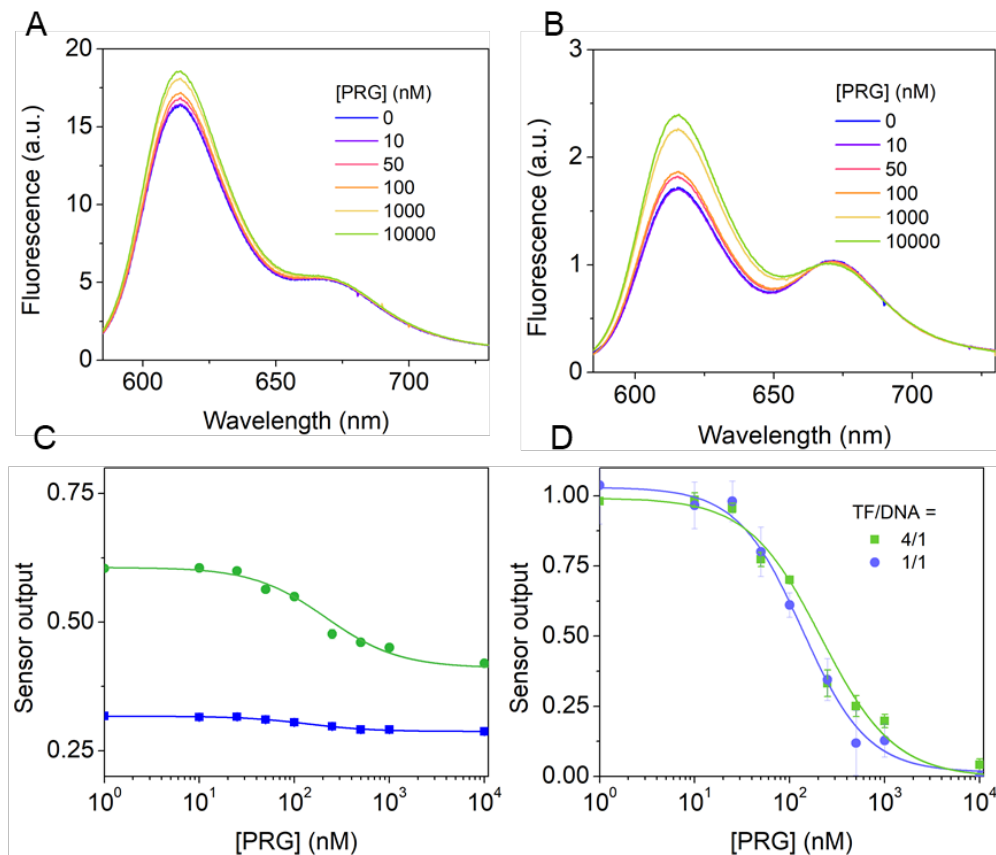
Figure S11. DNA2-TR to TF-Cy5 FRET sensor. A and B, fluorescence emission spectra (λ_{exc} = 550 nm) upon PRG addition with a ratio of DNA2-TR:TF-Cy5 =1:1 (A) and = 1/4 (B). C and D are the raw and normalized dose-response curve upon PRG addition. Data are mean ± standard deviation of n = 3.

TF-QD to DNA-Cy5
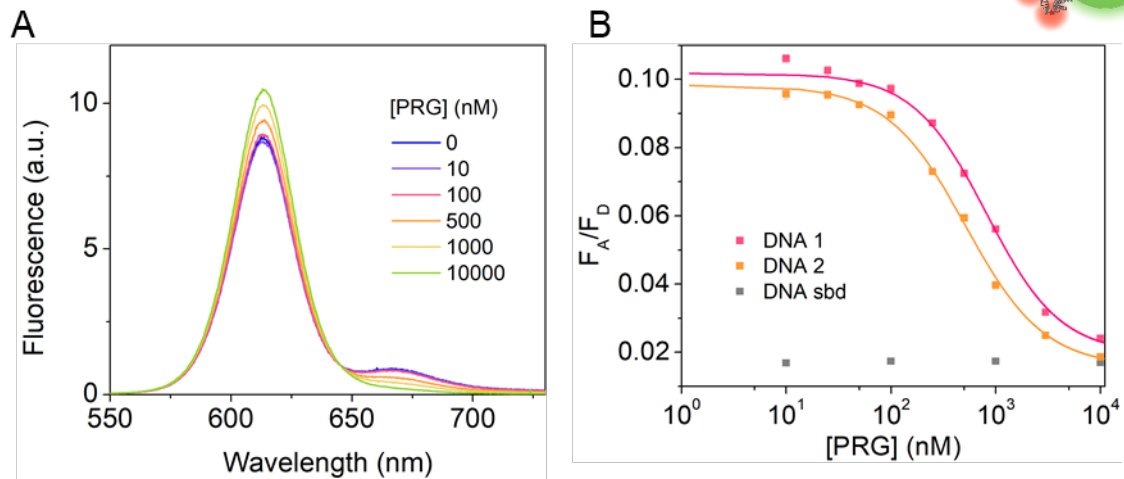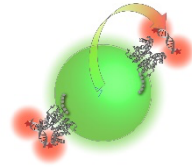
Figure S12. TF-QD to DNA-Cy5 FRET sensor. A. Fluorescence emission spectra (λ_{exc} = 550 nm) of TF-QD:DNA2-Cy5 (TF-QD:DNA-Cy5 = 4-1:16) upon PRG addition. B. Raw dose-response curve upon PRG addition of TF-QD:DNA1-Cy5, TF-QD:DNA2-Cy5 and TF-QD:DNAsbd-Cy5 (TF-QD:DNA-Cy5 = 4-1:16). Data are mean ± standard deviation of n = 3.

DNA-QD to TF-Cy5
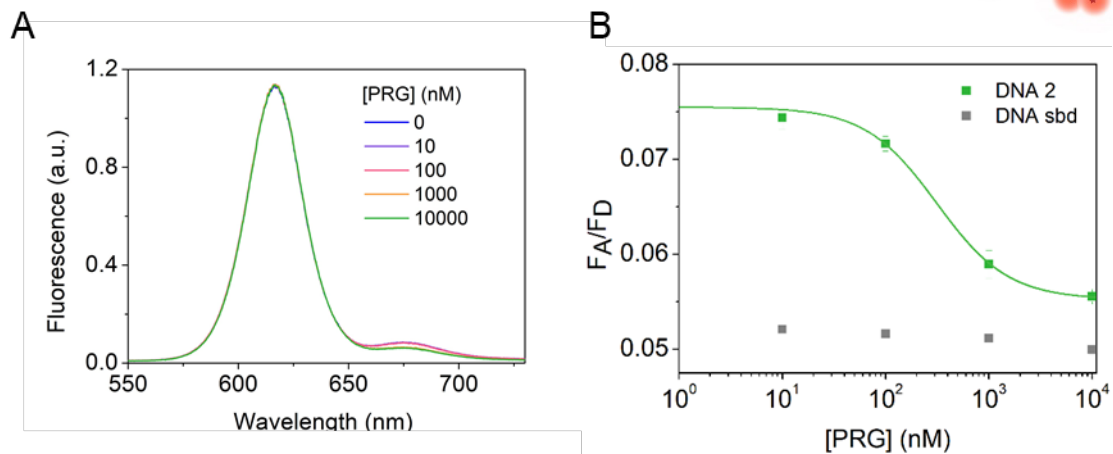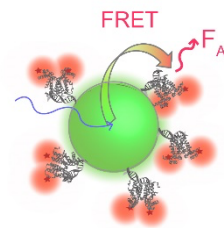
Figure S13. DNA-QD to TF-Cy5 FRET sensor. A. Fluorescence emission spectra (λ_{exc} = 550 nm) of DNA2-QD:TF-Cy5=18-1:18 upon PRG addition. B. Raw dose-response curve upon PRG addition of DNA2-QD:TF-Cy5 and DNAsbd-QD:TF-Cy5 (DNA-QD:TF-Cy5=18-1:18). Data are mean ± standard deviation of n = 3.

Sensor Simulations

We performed our sensor simulations in MATLAB using ode15s as the differential equation solver. This process requires a system of differential equations specific to each combination of sensor configuration and kinetic parameters. Therefore, we created a pair of modeler objects that initialize all relevant parameters and perform simulations, in addition to containing plotting functions to assist in visualization. The base object is a physical modeler, which initializes the time span to simulate over, a constant donor concentration, an array of acceptor concentrations to sweep over, and TF-dimer:DNA affinities to simulate. For each sensor configuration, we initialize a stoichiometric reaction matrix that indicates the number of a given species that are involved in a reaction, as well as their sign in the reaction, which indicates whether that species is produced or consumed, according to Equations 6-11. In a given simulation, we start by obtaining a set of initial species concentrations, as well as the forward and reverse reaction rates for each reaction. At each time step, the forward and reverse rates are multiplied by the current concentration of the appropriate species as per Eqs. 6-11, and the reverse value is subtracted from the forward value. These instantaneous reaction rates are stored in a rate vector, which is linearly combined with the stoichiometric matrix to generate the current rate of change for each species at a given time step. These rates serve as the input to ode15s, which runs across the provided time span, from 0 to 1 billion seconds, which empirically proved to be more than enough time for each simulation to reach equilibrium. Upon completion of a simulation, we take the average value of each species from the last 3 simulated time points (which controls for any potentially small fluctuations in concentration at the end) and store those in an NxM matrix, where N is the number of simulations performed, and M is the number of species in a given configuration. This stage of simulation allows us to generate plots displaying the fraction of donor species that are bound, and thus capable of emitting a FRET signal.

On top of this, we have built a FRET modeler that inherits from the base physical modeler, and is able to tune the fraction of bound donors into an actual FRET signal. This object begins by initializing a physical modeler for the donor/acceptor configuration of interest, and then retrieving FRET parameters specific to that configuration as described in Table S6. These FRET parameters are converted into an efficiency value for each acceptor:donor ratio in a configuration according to Equation 12, which is used to scale the fraction of bound donors into FRET signal. In our model, each of the parameters used to calculate R_0 (Eq. 13) were derived experimentally, leaving the Forster distance, r, as the lone free parameter for tuning FRET efficiency. Upon completion of these simulations, our modeling objects are able to

produce plots of each sensor swept across various TF-dimer:DNA affinities as shown in Figure 2.

Table S4: Reaction rates used in biophysical modeling, see figure 2. The TF-dimerization affinity (K_3) is an independent constant, while TF-monomer:DNA binding affinities (K_1, K_2) are dependent on the simulated TF-dimer:DNA affinity (K_4).

Variable	Description	Value
$K_{TFd:DNA}$ **(K_4)**	TF-dimer:DNA binding equilibrium constant	Sweep from 0.1nM to 0.1M, including the values from the experimentally determined DNAs
$K_{TFm:DNA}$ **(K_1)**	TF-monomer:DNA binding equilibrium constant	20 * $K_{TFd:DNA}$
$K_{TFm:TFDNA}$ **(K_2)**	TF-monomer:TFDNA binding constant (second monomer binding)	10 * $K_{TFd:DNA}$
$K_{TF\ dimerization}$ **(K_3)**	TF Dimerization equilibrium constant	100nM
$K_{TFd:DNA}$ **(Scrambled DNA K_4)**	Dimer:DNA binding constant for scrambled DNA	1μM

Table S5: FRET Parameters used in simulations. Values that were not experimentally determined in a given sensor configuration are *italic*. In the case of TF-monomer donors, we use the Quantum Yield of the DNA-donor, and for TF-monomer acceptors, we use the Spectral Overlap of TF-donors. These choices require us to recalculate R_0 for these configurations. The Forster distance, r, is tuned for each sensor configuration, such that each combination of sensor configuration & acceptor:donor ratio possesses its own FRET efficiency.

Donor	Acceptor	R0	Q_Y	J	r	FRET E
TF-TR	DNA-Cy5	*8.2nm*	*71*	2.29	*8.2nm*	*0.66*
TFTF-TR	DNA-Cy5	6.8nm	24	2.29	*8.2nm*	*0.25*
DNA-TR	TF-Cy5	*8.2nm*	*71*	2.29	*9.7nm*	*0.26*
DNA-TR	TFTF-Cy5	8.5nm	71	2.93	*9.7nm*	*0.48*
TF-QD	DNA-Cy5	6.6nm	25	1.76	*9.5nm*	*0.18*
DNA-QD	TF-Cy5	7.6nm	37	2.82	*11nm*	*0.0981 (n=1) - 0.7966 (n=36)*
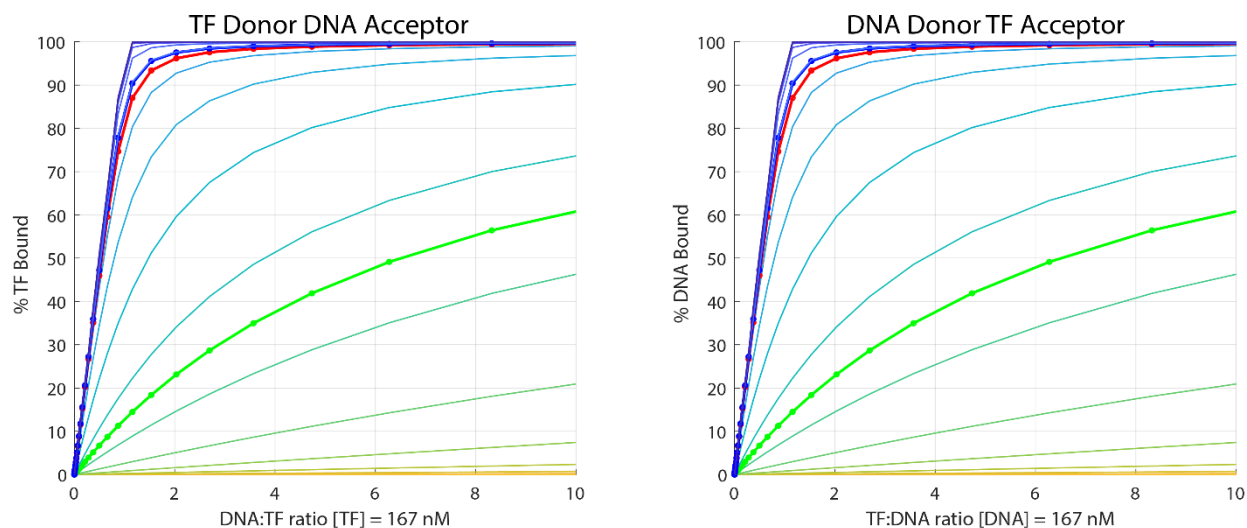
Figure S14 Traces of bound fractions in dye models without dimerization. These plots resulting from our simplest models do not capture the notable asymmetry between TF acceptor and donor as seen in our experimental results.

REFERENCES

1.   Holstein, C. A.; Griffin, M.; Hong, J.; Sampson, P. D., Statistical Method for Determining and Comparing Limits of Detection of Bioassays. Analytical Chemistry 2015, 87 (19), 9795-9801.
2.   Grazon, C.; Chern, M.; Ward, K.; Lecommandoux, S.; Grinstaff, M. W.; Dennis, A. M., A versatile and accessible polymer coating for functionalizable zwitterionic quantum dots with high DNA grafting efficiency. Chemical Communications 2019, 55 (74), 11067-11070.